

A model for the jet-disk connection in BH accreting systems

A. Hujeirat¹, and M. Livio²

¹*Max-Planck-Institut für Astronomie, 69117 Heidelberg, Germany*

²*SSTI, 3700 San Martin Drive, Baltimore, MD 21218, USA*

1 Abstract

The powerful and highly collimated jets observed in active galactic nuclei and μ -quasars are likely to be connected to the accretion phenomena via disks. Based on theoretical arguments and quasi-stationary radiative MHD calculations, a model for accretion-induced jet is presented. It is argued that accretion disks around BHs consist of 1) a cold, Keplerian-rotating and weakly magnetized medium in the outer part, 2) highly advective and turbulent-free plasma inside $r_{\text{tr}} = 10 - 20$ Schwarzschild radii, where magnetic fields (-MFs) are pre-dominantly of large scale topology, and in excess of thermal equipartition, and 3) an ion-dominated torus in the vicinity of the hole, where MFs undergo a topological change into a monopole like-topology. The action of MFs interior to r_{tr} is to initiate torsional Alfvén waves (-TAWs) that extract angular momentum from disk-plasma and deposit it into the transition layer (-TL) between the disk and the overlying corona, where the plasma is dissipative and tenuous. A significant fraction of the shear-generated toroidal magnetic field (-TMF) reconnect in the TL, thereby heating preferentially the ions up to the virial-temperature and forming a two-temperature, super-Keplerian rotating, centrifugal-accelerated ion-dominated outflows.

These gravitationally unbound outward-oriented motions serve as seeds, possibly, for all the powerful electron-proton jets observed in accreting systems containing BHs. Furthermore, the TMF in the TL is in thermal equipartition with the ions, whereas the poloidal component (-PMF) is with the electrons. Such a strong TMF is essential for increasing the jet-disk luminosity in the radio regime.

2 Introduction

Based on observational data, most of the systems containing jets are considered to be accreting systems, most likely with an accretion disk surrounding the central object. The most powerful and highly collimated jets are found to emanate from accreting systems containing, probably, black holes, with a maximum power attainable if the

central objects are Kerr BHs rotating at their maximum rate [7]. Beside the numerous extra galactic radio sources with high gamma-factors ($\gamma \geq 3$), the underlying engines powering the jets in microquasars such as GRS 1915 + 105 and GRO 1655 - 40 are believed to be spinning BHs [24].

Although there has been a significant progress in recent years toward understanding the morphology, propagation and shock diagnostics of jet-plasmas, no consensus has been reached yet about their basic driving mechanisms. Nevertheless, there are at least three ingredients that appear to be necessary for initiating jets that gained theoretical and observational supports: 1) large scale magnetic fields (-MFs), 2) an accretion disk and 3) a central object which dominates the disk gravitationally. Magnetic fields in particular are considered to play a major role in the evolution of jets. The fact that many jets have comparable radio and bolometric luminosities hints to the significant fraction of the magnetic energy in their total power.

In the first place MFs extract rotational energy from the underlying disk and deposit it into the plasma at higher latitudes, thereby initiating motions that are principally outward-oriented.

At relatively large radii MFs are pre-dominantly toroidal, and their main action is to force the rotating particles to collimate around the corresponding axis of symmetry. The central object must be relatively massive compared to the disk, so that its gravitational well is sufficiently deep for initiating motions with speeds comparable to the escape velocity near its surface.

In this paper we present a model for initiating jets from accretion disks around BHs. The model is a modified version of the truncated disks advective tori model (TDAT; [14], in which a special attention is given to the role of MFs.

Our approach relies on theoretical arguments supported by the radiative two-temperature MHD numerical calculations. The model is based on the following assumptions: 1) The Balbus-Hawley instability acts as dynamo that amplifies the unordered MFs up to thermal equipartition, 2) The Parker- and BH-instabilities in combination with reconnection close a dynamo cycle, through which a large scale MF is generated, in the manner that Tout& Pringle (1992) suggested. Once the large scale magnetic field becomes beyond thermal equipartition, the generation and dissipation of turbulence will be suppressed. 3) A significant fraction of the TMF-lines re-connects in the TL: a process which is treated by adopting a turbulent diffusivity η_{mag} , 4) Turbulent dissipation preferentially heats the the heavy particles rather than the electrons, so that the two-temperature description for the plasma can be applied[30].

Fig. 2 shows the main phases in the evolution of a accretion-induced jet. The paper runs as follows. In Sec. 3 we review several model for jet initiation, and outline the necessity for a new model. The structure of magnetized disk is discussed in Sec. 4. In sec. 5 the governing equations to be solved and the method of solution are described, while the corresponding results are presented in Sec. 6, and end up with the summary of the results in Sec. 7.

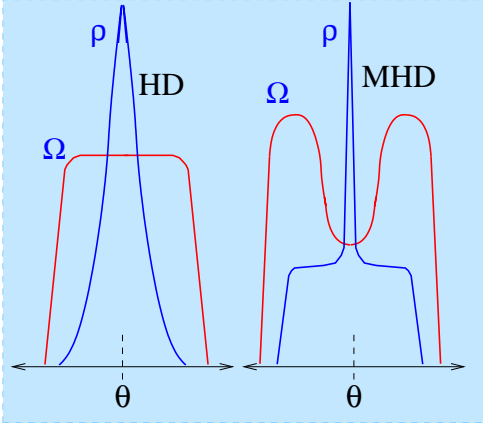


Figure 1: A schematic distribution of the rotational velocity Ω and density ρ across the disk with magnetic fields (MHD) and without (HD). The action of the equipartition MFs is to transport angular momentum from the disk to higher latitudes, where the particles are centrifugal-accelerated outwards.

3 The necessity for a new model

Several models have been suggested for initiating jets[19], [5], [28], [41], [34], [36], [21], [12], [8], [20], [17]. In the following we outline several properties of a few of these models:

1. The Blandford& Payne model (1982, henceforth BP82) relies on magnetic extraction of angular momentum and rotational energy from an underlying cold and Keplerian disk, i.e., from a standard disk (-SSD, [32]). Extraction is most efficient if the poloidal magnetic field is of a large scale topology and appropriately aligned to the disk-normal (i.e., the angle from disk-normal θ_B must be larger than 30°). The second important result is that, at large radii, collimation is achieved through the action of the shear-generated toroidal MF. The difficulties of this model are:
 - (a) The disk is infinitely thin. This implies that Lorentz forces exerted on the disk-plasma would force the inflow to rotate sub-Keplerian, making it difficult for the plasma to be flung out by purely centrifugal means[35]. Furthermore, taking into account that $B_T(z=0) = 0$ and adopting $\rho \sim r^{-3/2}$ as BP82 suggested, any dynamo cycle will not succeed to amplify B_p at $z=0$ to values beyond thermal equipartition. One possible way to obtain¹ $\beta > 1$ is through a collapse of the central part of the disk while

¹ $\beta = P_{\text{mag}}/P_{\text{gas}}$, where $P_{\text{mag}} = (B_p^2 + B_T^2)/4\pi$, see Eq. 8 for further details.

freezing its magnetic flux. In this case² $B_p \sim r^{-2}$, which implies that if B_p does not change topology, accretion will be terminated and the whole inflow will turn into outflow with unacceptably large mass load.

- (b) It has been argued that even if the poloidal MFs intersects the disk with $\theta_B > 30^\circ$, thermal assistance is still required for the disk-plasma to overcome the potential difference parallel to the MF-lines.
- (c) There is no special treatment to the flow in the deep gravitational well of the central object, which is necessary for increasing the total energy per gram of the inflow, and convert it into outflows with high speeds.
- (d) The model relies on ideal MHD treatment to a cold Keplerian disk. However, since $\beta \geq 1$, MFs will likely suppress the generation and dissipation of turbulence. Hence, the disk is likely to be thermal unstable. If the accretion rate is high, the disk becomes optically thick to Synchrotron/cyclotron radiation; gyrating electrons emit radiation on the cyclotron frequency, that in turn repeatedly upscattered by the hot electrons, establishing thereby a thermal equilibrium. Since this occurs on a time scale comparable or even shorter than the dynamical one, and in the absence of other efficient heating sources, the disk undergoes a runaway cooling: the temperature decreases and reach the lower limit $T_{\min} = h\nu_{\text{peak}}/k$, where ν_{peak} is the peak cyclotron frequency. This thermally induced collapse of the inner disk gains acceleration if the accretion rate is low. Here the low frequency photons emitted by the gyrating electrons escape from the system without being absorbed or scattered, and so no lower limit for the temperature can be constructed.

2. The X-wind model (Shu et al. 1994). Here the magnetically driven-wind emanate, neither from the disk nor from the central object, but from the region around the co-rotation radius, r_{cor} , where the effective gravity vanishes. The model relies primarily on the poloidal MFs of the central object which is surrounded by an accretion disk, essentially without large scale magnetic fields. This approach relaxes the winding up problem of the poloidal MFs, which has been encountered in the Ghosh & Lamb model (1979). Moreover, as outflows here originate from the region close to the surface of the star, their propagation speed is estimated to be of the order of the escape velocity.

When extending this model to accretion flows around BHs, the following problems arise:

- (a) It is not applicable to accretion flows onto Schwarzschild BHs, as these objects do not possess dynamically stable poloidal MFs. If such holes are

² $\Phi = 2\pi r^2 B_p \approx 2\pi r^2 B_\theta = \text{const.}$

viewed as extreme stars, then the X-wind model rule out indefinitely the possibility of jet initiation from weakly magnetized slowly rotating objects.

- (b) Balbus & Hawley instability amplifies weak MFs up to approximately thermal equipartition on the dynamical time scale. In the innermost region of the disk, MFs of the central object are beyond super-equipartition with respect to the thermal energy of the disk-plasma; generation and dissipation of turbulence will be suppressed, the plasma in the X-region (see Fig. 2b in [36]) becomes cold, and the radial accretion will be terminated.
- (c) Almost all young stellar objects have been observed to rotate far below the beak-up velocity. Although the FU Orinois objects accrete at relatively high rates, they are considered to be slow rotators. Fast rotators, however, show excessive magnetic activities, which is in line with the Parker instability[37]. In the X-wind model however, MFs in the X-region are nearly in equipartition with the potential energy of the flow. Such strong magnetic tubes are likely to be gravitationally unbound, cannot be anchored deep in the star and therefore they float upwards to the surface on the dynamical time scale. This occurs if they are generated in the convection zone or in the overshoot layer between the convection zone and the underlying rigidly rotating core, similar to the solar dynamo[38].

3. Advection-dominated inflow outflow solutions -ADIOS (Blandford & Begelman 1999),

ADIOS are special case of ADAF solutions (advected dominated accretion flows) in which the accretion rate is allowed to adopt the self-similar profile $\dot{M} \sim r^p$, where $0 \leq p \leq 1$. Thus, the accretion rate decreases inwards, thereby giving rise to a substantial outflow with large mass load. ADIOS model is another step closer than ADAF toward explaining the low luminosity AGNs. Indeed, there are several numerical calculations that confirm the inward decrease of the accretion rate (e.g., [39]). However, these calculations did not rule out the possibility that the outflows obtained might be large scale circulation. On the other hand, in addition to the difficulties associated with ADAF solutions, ADIOS model:

- (a) relies on one dimensional treatment to an intrinsically multi-dimensional phenomenon. The model does not provide answers to numerous questions related to jet-morphologies, such as the origin of the high speed of jet-propagation, the role of the central object, the magnetic field topology appropriate for initiating jets and etc.
- (b) It largely overestimates the mass load of jets. Basically, it predicts that almost all accreted matter through the disk at large radii will re-appear in the jet. When applied to the galactic center, an accretion rate that is about

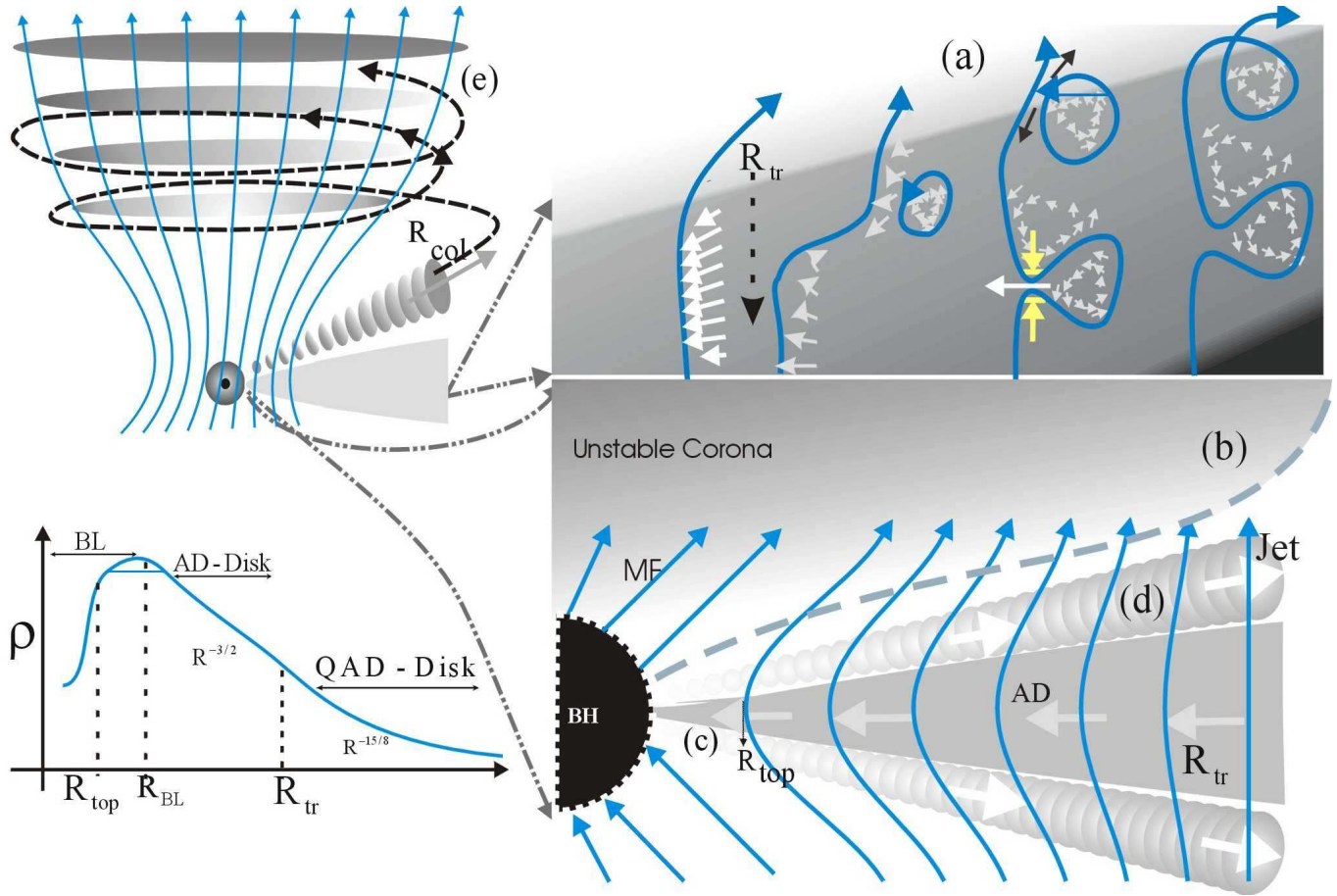


Figure 2: A schematic illustration of the jet-disk connection. In the outer region of the disk MFs are weak and advected-around MFs by the fluid motions. BH- and Parker instability in combination with reconnection and inwards accretion amplified the MFs up to thermal equipartition. The MFs become of large scale topology and truncate the disk at r_{tr} into advection-dominated (part a). Interior to r_{tr} (b), turbulent-generation and dissipation are suppressed, and TAWs become the dominant angular momentum transporter (c). TAWs carry angular momentum from the disk and deposit it into the thin layer above, where ions rotate super-Keplerian, virial-heated by reconnection of the TMF-lines, and start to centrifugal-accelerate outwards (part d). The ions in the TL are associated with internal, rotational and TMF-energy to start collimation at r_{col} , where the magnetic-diffusivity becomes vanishingly small (part e). For clarity, a schematic description of the density profile versus radius of the model is shown.

one order of magnitude larger than the upper limit would be necessary to obtain a partial fitting with the observed SED (Yuan et al 2002). Furthermore, neither ADAF nor ADIOS models are able to reproduce reasonable SED-fitting with observations in the radio frequency regime. They seriously underestimate the radio luminosities in AGNs and black hole X-ray transients[10],[9].

- (c) The dynamical range of ADIOS is largely overestimated. To clarify this point, let r_{tr} be the transition radius, at which an SSD makes a transition to ADAF (Fig. 2). If both solutions are thermally and dynamically stable, why should an SSD change into ADAF at large radii, or vice versa?

Mathematically: in the absence of external forces and for given Dirichlet boundary conditions, there is at most a single weak solution to the set of the corresponding linear systems of equations, which fulfils the entropy principle. Accordingly, at large radii the system of equations are nearly linear (i.e., they can be linearized as there are no mechanisms for generating shocks or strong gradients), and the conditions imposed at the outer boundary determine the solution uniquely. Note that the equations describing accretion flows in SSD or ADAF are predominantly Eulerian, except the angular momentum and energy equations that contain second order partial differential operators³. For example, if we set the angular velocity at the outer boundary to be sub-Keplerian and replacing L_E by Λ_B (see Eq. 12), the SSD changes to ADAF. However, since there is no reason to expect an excessive source of heating at large radii, as in ADAF case, only cold standard disks are likely to survive there. These disks continue to maintain their thin geometrical structures all the way down to the central object, where other effects come into play, e.g., heat conduction, change of the MF-topology, noticeable change of rotation-law and manifestation of the magnetic field and the gravitational well of the central object. Indeed, Abramowicz et al. (1998) concluded that a transition from SSD to ADAF may occur in the vicinity of the BH. Hujeirat & Camenzind (2000a) found that the transition is thermally unstable, and the plasma in the outermost part of ADAF collapses dynamically, thereby extending the SSD down to several last-stable radii, where the disk truncates and an ion-dominated and highly eddy torus emerges.

An additional evidence that rules out transitions at large radii are MFs. ADAF/ADIOS models assume that MFs are in equipartition with the thermal energy. If this is the case, then this should apply also when MFs are

³In spherical geometry they read $L_E = \nabla \cdot \lambda_{\text{FLD}} \nabla E$, and $L_\ell = \nabla \cdot \eta_{\text{tur}} \nabla \Omega$, respectively. E and λ_{FLD} are the radiation density and the radiative diffusion coefficient as defined in Eq. 12, Ω and η_{tur} the angular frequency and coefficient of turbulent diffusion, respectively.

of large scale topology. However, since the accretion flow is fully ionized and freely falling, magnetic flux freezing implies that the MF-strength will strongly increase inwards and become in equipartition with the potential energy of the flow, hence terminating accretion. This impose a constrain on the location of the transition radius: r_{tr} must be smaller than 10 – 20 last-stable radii, depending on the accretion rate.

4. Truncated disks - advective tori solution (TDAT, Hujeirat & Camenzind 2000b). The model relies on the results of radiative HD calculations of two-temperature accretion flows onto BHs without magnetic fields. This important results of TDAT read: 1) the disk truncate close to the last stable orbit, and forms an ion-dominated highly advective torus, 2) outward-oriented motions of plasmas between the disk and the overlying corona are formed, and which are manifested when MFs are included[17]. In this paper, the previous model [17] is presented in details, and its astrophysical capability to reproduce the spectral energy distribution of the jet in M87 is confirmed.

4 Disk structure and magnetic braking

4.1 The outer part

In SSDs the inward-advection of angular momentum is balanced by outward viscous transport. This is equivalent to equalize the terms T0 and T3 in Eq. 1, while all other terms are neglected.

$$\frac{\partial \ell}{\partial t} + \overbrace{\nabla \cdot V \ell}^{\text{T0}} = \overbrace{B_r \frac{\partial r B_T}{\partial r}}^{\text{T1}} + \overbrace{B_\theta \frac{\partial B_T}{\partial \theta}}^{\text{T2}} + \overbrace{\frac{1}{r^2} \frac{\partial}{\partial r} r^4 \rho \nu \frac{\partial \Omega}{\partial r}}^{\text{T3}} + \overbrace{\frac{1}{\cos \theta} \frac{\partial}{\partial \theta} \cos \theta \rho \nu \frac{\partial \Omega}{\partial \theta}}^{\text{T4}}. \quad (1)$$

T0 denotes angular momentum transport via advection, T1 and T2 are for magnetic extraction, and T3 and T4 are for viscous (micro- or macroscopic hydrodynamical turbulence) re-distribution of angular momentum.

The key question here is how the constellation of these terms would look like in the vicinity of the black hole.

In the outermost regions of a disk, we anticipate magnetic fields to be below equipartition. Let r_{tr} be a transition radius (see Fig. 2), such that for $r > r_{\text{tr}}$, we have the usual SSDs, where the ratio of magnetic to gas pressure is $\beta \ll 1$. Here the Balbus-Hawley instability [2] operates on the dynamical time scale: it rapidly amplifies the MF and forces β to approach, but remains below, unity [11]. On the other hand, the rotational energy in SSDs exceeds the thermal energy by at least one order of magnitude. Therefore, the generated toroidal magnetic energy via shear can easily exceed thermal equipartition. Consequently, unless the imposed boundary conditions

limit the amplification of the TMF, there is no reason to expect β to remain strictly below unity.

4.2 The inner part

Whether the disk is surrounding compact object or a YSO, the innermost part of the disk is likely to be strongly magnetized. The question which then arise is: how does accretion onto BHs proceed under $\beta \geq 1$ condition?

In general, accretion via strongly magnetized and turbulence-free disks proceeds if the MFs are able to extract angular momentum from the rotating disk-plasma. The efficiency of this extraction depends, among others, on the MF-topology. For example, large scale or dipolar MF-topologies are considered to be appropriate for extracting rotational energy from the disk or even from the hole itself and power jets. In the present study, MFs are assumed to be of large scale topology. This is reasonable, as the BH-instability in combination with the Parker instability may establish a dynamo cycle in which the inward-advected and initially weak MFs are amplified and then reconnect to build up the desired MF-configuration[40]. A straightforward conclusion that can be drawn is that when the matter at the outer region has completed one revolution around the central BH, MFs should have reached equipartition almost everywhere in the disk. This would eventually suppress self-generated turbulence and terminating angular momentum transport through turbulence-friction.

In the region $r < r_{\text{tr}}$, global conservation of the poloidal magnetic flux implies that $B_{\text{p}} \sim r^{-2}$. Therefore, as the innermost part of the disk contracts, there would be a critical radius r_{top} below which gravitational-equipartition is maintained, eventually terminating accretion. This configuration is unlikely, as this would imply that most of accretion inflow would be re-directed into outflow, with an unacceptably large mass load. On the other hand, if r_{top} is sufficiently close to the last stable orbit, a change of the MF-topology associated with a significant loss of magnetic flux through the horizon would be possible. This is a plausible event, as MFs close to the horizon are unlikely to adopt other than a monopole like-topology (see Fig. 2/b). Under such circumstances, the generation of B_{T} will be considerably reduced and the accretion of matter within r_{top} proceeds unhindered.

Around the radius r_{top} angular momentum transport is mediated through magnetic braking. When combining Eq.1 with the equation corresponding to the time-evolution of the TMF (see Eq. 8), and assuming the flow to be locally incompressible, we obtain a magnetic torsional wave equation which has the approximate form:

$$\frac{\partial^2}{\partial t^2} B_{\text{T}} \cong V_{\text{A}}^2 \Delta B_{\text{T}}. \quad (2)$$

Δ denotes the two-dimensional Poisson operator in spherical geometry, and V_{A} ($\doteq B_{\text{p}}/\sqrt{\rho}$) is the Alfvén speed. The action of these waves is to magnetic brakes the

innermost part of the disk through transporting angular momentum from the disk to higher latitudes. Note that B_p determines uniquely the speed of propagation, hence the efficiency-dependence of angular momentum transport on the B_p -topology. These TAWs propagate in the vertical direction on the time scale:

$$\tau_{\text{TAW}} \sim \frac{H}{V_A} \sim \tau_{\text{dyn}}.$$

This should be similar to the removal time scale of angular momentum from the disk⁴:

$$\tau_{\text{rem}} \sim \rho V_T H / B_P B_T \sim r^{3/2}. \quad (3)$$

Thus, τ_{rem} increases non-linearly with radius, attaining a minimum value at the inner boundary. This implies, for example, that the rate at which angular momentum is removed at the last stable orbit ($\doteq R_{\text{LSO}}$) is one thousand times faster than at $r = 100R_{\text{LSO}}$. To avoid the innermost region of the disk from running out of angular momentum, we require the disk to be dynamically stable. Equivalently, the rate at which angular momentum is removed at any radius must be equal to the rate at which it is advected inwards from outer layers, i.e., $\tau_{\text{adv}} = \tau_{\text{rem}}$. This implies that the radial velocity $-U$ in the disk is of the order of the Alfvén speed, which is also of the order or even larger than the sound speed V_S , hence the terminology advection-dominated disk.

The question which arises here is whether the disk, under these circumstances, maintains its geometrical thin structure.

The answer is hidden in the vertical momentum and energy equations. The former reads:

$$\frac{\partial V}{\partial t} + V \cdot \nabla V = \frac{1}{\rho r} \frac{\partial P}{\partial \theta} + \tan \theta \frac{V_\varphi^2}{r} + \frac{\nabla \times \nabla \times B}{4\pi\rho} \Big|_{\vec{\theta}}. \quad (4)$$

Taking into account that vertical transport of angular momentum is maintained through magnetic braking nearly without particle-advection (i.e., we neglect the second term in the LHS of the equation), and noting that $(\partial P / \partial \theta) / r \rho$ is the only term that opposes the vertical contraction of the disk, we obtain:

$$\frac{H}{r} \approx \frac{V_S}{V_\varphi}. \quad (5)$$

This implies that, as in SSDs, the thickness of the disk depends strongly on the temperature of the plasma, and hence on the associated heating mechanisms. On the other hand, since $\beta \geq 1$ in the innermost part of the disk, the dominant source of heating in SSDs (i.e., turbulence dissipation), is no longer efficient. In this case, heating is mainly due to adiabatic compression and to other non-local sources, e.g.,

⁴ τ_{rem} is obtained from the terms T0 and T2 in Eq. 1

radiative reflection, Comptonization and conduction of heat flux from the surrounding media. However, these mechanisms are unlikely to change the disk configuration significantly, so that the disk continue to maintain its thin geometrical structure. Specifically, for $r \leq r_{\text{tr}}$, we have $\partial H_{\text{d}}/\partial r \geq 0$.

4.3 Formation of the ion-dominated torus

Whether the disk model is an SSD, ADAF or ADIOS, most of the physical variable (e.g., density temperature, radial and angular velocities) increase with decreasing radius. On the other hand, the disk is said to be truncated if within a certain radius, say r_{BL} , part of the main physical variable start to decrease inwards. This occurs, for example, if the central object rotates sub-Keplerian⁵. The Kepler-rotating and inflowing material from the disk must release a significant fraction of its angular momentum to be able to cross the event horizon of a Schwarzschild BH. This might be achieved if the MFs in the BL are sufficiently strong to extract angular momentum from the disk on the dynamical time scale. However, this requires the density to decrease considerably inwards, so that the speed of propagation of the TAWs largely exceeds that in the outer disk.

We note that, unlike SSD and ADAF-models that predict a density-decrease with radius (i.e, $\rho \sim r^{-15/8}$ and $\rho \sim r^{-3/2}$, respectively), hydro- and MHD-calculations show, indeed, an inwards decrease of the density in the BL[13],[39], [27].

In SSDs the pressure gradient ∇P_{gas} is neglected, whereas in ADAF the pressure adopts the profile $p \sim r^{-5/2}$. When comparing the gravitational to the advective time scale at the inner boundary, it is easy to find that the rate of advection increases inwards, forcing thereby the density to be minimum at the inner boundary. As a consequence, the in-flowing material at r_{BL} experiences a pressure-induced acceleration. Taking into account that the Coulomb coupling between the ions and electrons is $\Lambda \propto \rho^2$, thermal decoupling may occur, and formation of an ion-dominated torus is an inevitable phase in the evolution of accretion flows onto BHs.

How does heat conduction affect the structure of the ion-torus?

Generally, the temperature of both the ions and electrons increase inwards. The effect of heat conduction is to transport heat from hot into cold plasma, i.e, from inside-to-outside. In the absence of magnetic field and assuming the mean turbulent motion to be proportional to the sound speed, the innermost part of the disk will be evaporated by heat conduction of the ions, and therefore the torus starts to expand outwards [14]. When large scale MFs are taken into account, the torus contracts rather than expands. The reasons are: 1) heat conduction operate parallel to the MF-lines, and 2) strong MFs act to diminish the generation and dissipation of turbulence.

Unlike stars that heat up the surrounding media, BHs are heat-absorber (the sur-

⁵This applies for Kerr black holes with $a < 1$.

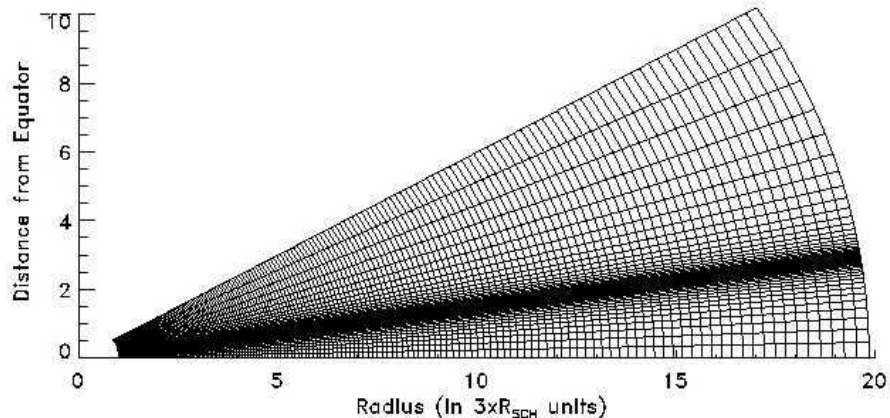


Figure 3: A partial display of the distribution of 220 and 100 finite volume spherical cells in the radial and horizontal directions that covers the domain of calculations. Highly refined mesh distribution is adopted in the transition layer, where most of the physical variable undergo a strong spatial variation and where jet-launching occurs. The aspect ratio adopted here, i.e., the ratio of the finest volume cell to the largest one, is $\approx 10^4$.

rounding corona is not heated from below). Therefore, the ion-dominated torus contracts and may survive in the vicinity of the last stable orbit only, where MFs are pre-dominantly of large scale topology.

In addition, the location of r_{tr} depends strongly on the accretion rate \dot{M} . A large \dot{M} enhances the Coulomb coupling, reduces the effect of heat conduction and thereby slowing the propagation speed of the TAWs (which reduces the efficiency of the magnetic braking). Thus, the volume of the ion torus shrinks and the total power injected into the jet-plasma decreases accordingly.

5 The governing equations

When modelling flow-configurations in the vicinity of a BH, it is necessary to use spherical geometry. Since the dynamical time scale close to the last stable orbit is extremely short, thermal decoupling between the electrons and the protons is possible. In this case, the set of equations to be solved consists of the continuity equation:

$$\frac{\partial \rho}{\partial t} + \nabla \cdot (\rho \vec{V}) = 0, \quad (6)$$

the three momentum equation for the material flux:

$$\frac{\partial \vec{M}}{\partial t} + \nabla \cdot (M \otimes \vec{V}_i) = -\nabla P_g + \mathbf{f}^{grav,cent,rad} + \frac{\nabla \times B \times B}{4\pi} + Q^{\text{visc}}, \quad (7)$$

where ρ , $\vec{V} = (V_r, V_\theta, V_\varphi)$, \vec{M} and P are the density, velocity vector, material flux $\vec{M} = \rho \vec{V}$, and gas pressure $P (\doteq \mathcal{R}_{\text{gas}} \rho (T_i/\mu_i + T_e/\mu_e))$. The subscripts “i” and “e” correspond to ions and electrons. $\mu_i = 1.23$ and $\mu_e = 1.14$. $\mathbf{f}^{grav,cent,rad}$ is the force vector which includes the gravitational, centrifugal and radiative forces. Quasi-Newtonian gravity is used to describe the gravity of the central BH [29]; Q^{visc} denotes the collection of second order diffusive operators.

The evolution of the MFs is followed by solving the induction equation which reads:

$$\partial_t \vec{B} = \nabla \times (\vec{V} \times \vec{B} - \eta_{\text{mag}} \nabla \times \vec{B}). \quad (8)$$

Here, $\vec{B} = (B_r, B_\theta, B_\varphi) = (B_p, B_T)$. To quench the amplification of the TMF in the TL, we adopt the magnetic turbulent diffusivity: $\eta_{\text{mag}} = \alpha V_{\text{AT}} H_d$, where $V_{\text{AT}} = B_T/\sqrt{\rho}$. In solving this equation for \vec{B} , the solenoidal condition $\nabla \cdot \vec{B} = 0$ must be satisfied everywhere and for all times [15].

The dynamical time scale in the innermost region of the disk is sufficiently short, that thermal decoupling between the electrons and ions is inevitable [30], [25]. To take this possibility into account, both equations describing the thermal evolution of the ions and electrons should be solved. In this formulation, the bulk of heat generated by turbulent dissipation goes into heating mainly the ions in virtue of their large mass compared to the electrons. The dominant cooling mechanisms for the ions are conduction and two-body interaction with the electrons. The electrons, on the other hand, are subject to various cooling processes, e.g., Bremsstrahlung, Comptonization, Synchrotron and conduction. Surprisingly, ion-conduction appears to play an important role in the innermost region of the disk, where the ions form an ion-dominated torus and evaporate the inner part of the disk [14].

Under these conditions, the respective internal energy equations of the ions and electrons read:

$$\frac{\partial \mathcal{E}^i}{\partial t} + \nabla \cdot (\mathcal{E}^i \vec{V}) = P^i (\nabla \cdot \vec{V}) + \nabla \cdot [\kappa_{\text{cond}}^i \nabla T_i] + \mathcal{D} - \Lambda_{i-e}, \quad (9)$$

$$\frac{\partial \mathcal{E}^e}{\partial t} + \nabla \cdot (\mathcal{E}^e \vec{V}) = P^e (\nabla \cdot \vec{V}) + \nabla \cdot [\kappa_{\text{cond}}^e \nabla T_e] + \Lambda_{i-e} - \Lambda_B - \Lambda_C - \Lambda_{\text{syn}} \quad (10)$$

where $P^{e,i} = \mathcal{R}_{\text{gas}} \rho (T_i/\mu_i, T_e/\mu_e)$, $\mathcal{E}^{e,i} = P^{e,i}/(\gamma - 1)$ and $\gamma = 5/3$. \mathcal{D} , Λ_B , Λ_{i-e} , Λ_C , Λ_{syn} are the turbulent dissipation rate, Bremsstrahlung cooling, Coulomb coupling between the ions and electrons, Compton and synchrotron coolings, respectively. Here,

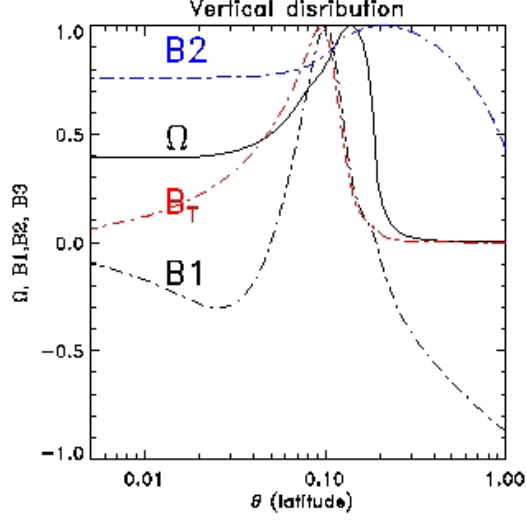


Figure 4: The horizontal distribution of the normalized angular velocity Ω , the PMF-components $(B1, B2) = (B_r, B_\theta) = B_P$ and the TMF (B_T) at $r = 2.5$. Note the super-Keplerian rotation and the strongly enhanced strength of the MF-components in the TL.

we use the following express:

$$\Lambda_{i-e} = 5.94 \times 10^{-3} n_i n_e c k \frac{(T_i - T_e)}{T_e^{3/2}}$$

$$\Lambda_B = 4ac\kappa_{\text{abs}}\rho(T^4 - E),$$

$$\Lambda_C = 4\sigma n_e c \left(\frac{k}{m_e c^2}\right) (T_e - T_{\text{rad}}) E,$$

where κ_{abs} and σ are the absorption and scattering coefficients. n_e , n_i the electron- and ion-number densities. The radiative temperature is defined as $T_{\text{rad}} = E^{1/4}$, and E is the density of the radiative energy in the zero-moment approximation of the radiative field. For the synchrotron cooling function, the following relation is adopted[31]:

$$\Lambda_{\text{syn}} = \frac{E_{\text{mag}}}{E} \Lambda_C, \quad (11)$$

where E_{mag} , E are the magnetic and radiative energies, respectively.

The second order operators on the RHS of Equations (9) and (10) are conductive operators and the conduction coefficients in cgs units read (Sandbæk & Leer 1994):

$$\kappa_e = 7.8 \times 10^{-7} T_e^{5/2}, \quad \kappa_i = 3.2 \times 10^{-8} T_i^{5/2}$$

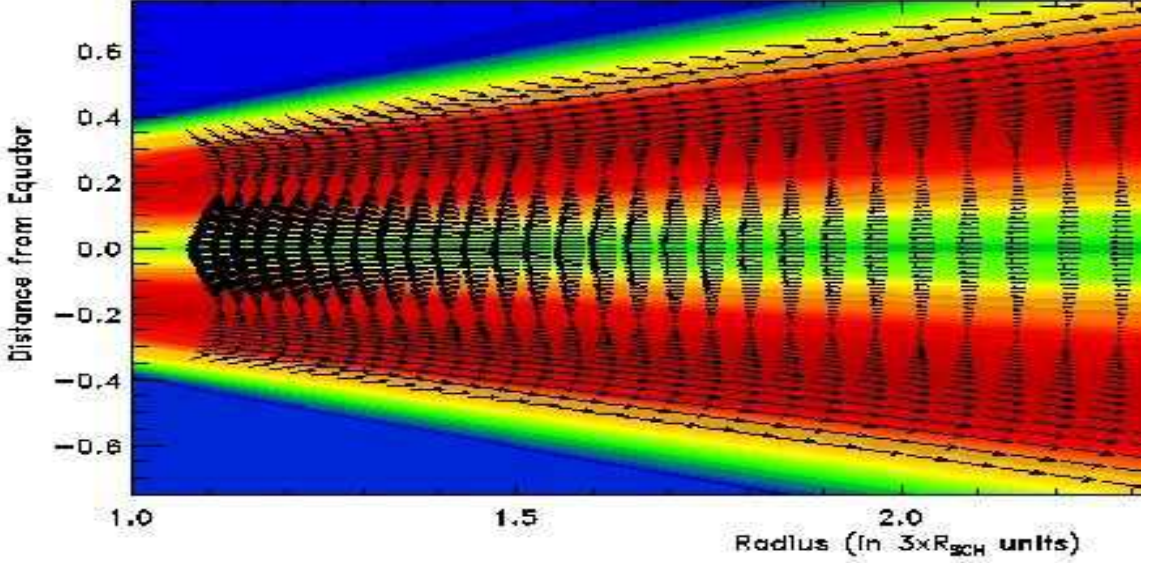


Figure 5: The distribution of the velocity field in the innermost part of the disk, superposed on the logarithmic-scaled ratio of the ion- to electron-temperatures (red color corresponds to high ratios and blue to low-ratios).

To follow the evolution of the radiative field, several assumptions have been made. Mainly, it is assumed that the field is isotropic and that the Flux-limited-Diffusion (FLD) approximation can be used to close the set of radiative moments. Thus, only the 0-moment equation of the radiation field is solved. Since the optical depth in the disk can be large in certain regions, and small in others, FLD approximation is used to model the radiative flux appropriately in these different regions, and to assure the monotonicity of the flux in the transition regions in-between. The 0-moment of the radiation field then reads:

$$\frac{\partial E}{\partial t} + \nabla \cdot (E\vec{V}) = \nabla \cdot [\lambda_{\text{FLD}}\nabla E] - \Lambda_B + \Lambda_C + \Lambda_{\text{syn}}, \quad (12)$$

where λ_{FLD} is flux limited diffusion coefficient which forces the radiative flux to adopt the correct form in optically thin and thick regions, i.e.,

$$\nabla \cdot \frac{\lambda_{\text{FLD}}}{\chi} \nabla E = \begin{cases} \nabla \cdot \frac{1}{3\chi} \nabla E & \text{if } \tau \gg 1 \\ \nabla \cdot nE & \text{if } \tau \ll 1, \end{cases} \quad (13)$$

and provides a smooth matching in the transition regions. Here $\chi = \rho(\kappa_{\text{abs}} + \sigma)$ and $n = \nabla E / |\nabla E|$.

5.1 Method of solution, initial and boundary conditions

The solution procedure is based on using the implicit finite volume solver IRMHD3 to search steady-state solution for the above-mentioned 3D axi-symmetric, two-temperature, diffusive, radiative and MHD equations in conservative form [15].

We note that the strong non-linearities governing these equation may not admit steady state, but strongly time-dependent or, in the best cases, quasi-stationary solutions. This implies that the terms describing the time-variation of the variables, i.e., $\partial/\partial t$, must be retained. On the other hand, since the dynamical time scale for accretion flows is shortest at the inner boundary, searching for quasi-stationary for the global flow-configuration on these time scales could be a computationally prohibitive process. To overcome this problem, we use the following spatially varying time stepping (-SVTS) approach, in which

$$\delta t_i = \alpha \delta r_i, \quad (14)$$

where δt_i , δr_i are the time step size and the radial mesh increment of a finite volume cell at a given radius r_i . The coefficient α is a constant of order unity.

This SVTS method is appropriate for searching quasi-steady configuration of accretion flows or ebeb for the collapse of cloud cores in molecular clouds, in which the radial grid points are non-linearly distributed and δr increases with radius. If δr is constant, then α must depend on the radius. In this case we suggest $\alpha = \alpha_0(r/r_{\text{in}})$, where α is a constant of order unity and r_{in} is the radius at the inner boundary.

The main disadvantageous of SVTS method is its inability to provide time scales for features that possess quasi-stationary behaviour, and that might be of astrophysical relevance. Here we suggest to use the obtained quasi-stationary solutions as initial configuration and re-start the calculations using a uniform time step size.

We note that SVTS method can be applied to explicit numerical methods as well. Here the global Courant number should be replaced by a local one, so that each finite volume cell has its own time step size.

In the present paper, the equations are solved in non-dimensional form, using the reference scaling variables: $\tilde{\rho} = 2.5 \times 10^{-12} \text{g cm}^{-3}$, $\tilde{T} = 5 \times 10^7 \text{K}$, $\tilde{U} = \tilde{V}_S = \gamma \mathcal{R}_g \tilde{T} / \mu_i$, ($\mu_i = 1.23$). $\tilde{B} = \tilde{V}_S \sqrt{4\pi \tilde{\rho}}$. The location of the transition layer (-TL), where the ion-dominated plasma is expected to rotate super-Keplerian and centrifugal-accelerated into jets, is shown in Fig. 2 for clarity.

The central object is taken to be a $10^8 M_\odot$ Schwarzschild BH. The domain of calculations is the quadrant: $D = [0 \leq \theta \leq \pi/2] \times [1 \leq r \leq 20]$. Radii are given in units of the inner radius $R_{\text{in}} \doteq 2.8 R_S$, where R_S denotes the Schwarzschild radius $R_S \doteq 2GM/c^2$. Through the outer boundary and within the thickness $H_d = 0.1r$, the constant accretion rate $\dot{\mathcal{M}} = 0.01 \times \dot{\mathcal{M}}_{\text{Edd}}$ is assumed. The inflow-temperature is taken to be $T = 10^{-3} T_{\text{virial}}$. The ion-temperature T_i is set to be equal to the electron temperature T_e initially. A hot and tenuous corona ($T = T_{\text{virial}}$, and density

$\rho(t = 0, r, \theta) = 10^{-4}\rho(t = 0, r, \theta = 0)$ is set to sandwich the disk.

Across the inner boundary, free-fall for the radial velocity and stress-free conditions for the angular velocity are imposed. Normal symmetry and anti-symmetry conditions are assumed along the equator and along the polar axis. The domain of integration is divided into 220×80 strongly stretched finite volume cells in the radial and vertical directions, respectively (Fig. 3).

Special attention was given to the physical consistency of the imposed conditions that MFs must fulfil at the inner and outer boundaries. This is especially important in magnetic-diffusive plasma, as second order magnetic diffusive operators may allow informations to be communicated between the inner and outer boundaries on the dynamical time scale. Therefore, magnetic stress-free conditions have been imposed at both boundaries. This is equivalent to require $\nabla \times B = 0$. Thus, the magnetic diffusive operators vanish at the inner and outer boundaries, which is a reasonable assumption for accretion-disk inflows around BHs, in which the magnetic Reynolds numbers can be extremely large in certain regions and small in others.

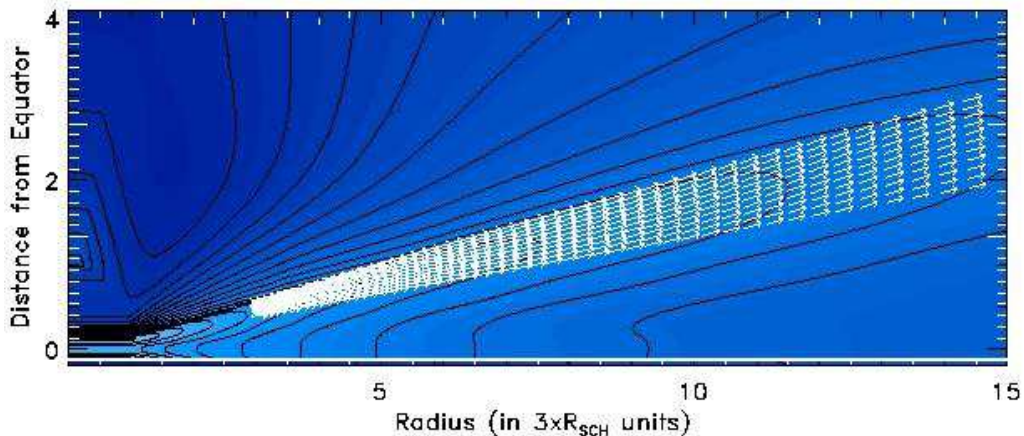


Figure 6: The distribution of the velocity field in the transition region superposed on equally-spaced isolines of the angular velocity Ω . The strong-decrease of Ω with radius in the equatorial region relative to its slow-decrease in the TL is obvious.

6 Results: formation of the super-Keplerian layer

When an isolated Keplerian-rotating particle in the equatorial near-plane is shifted to higher latitudes while conserving its angular momentum, its rotation becomes super-Keplerian locally, and therefore it starts to move outwards. Moreover, noting that τ_{TAW} decreases strongly inwards, a transition layer between the disk and the hot tenuous corona starts to form from inside-to-outside, where the matter rotates

super-Keplerian. Based on a previous calculations [17], it was found that that: 1) the angular velocity in the TL adopts the approximate power law profile $\Omega \sim r^{-5/4}$, 2) ions cool predominantly through fast outflows, and 3) the amplification of the generated TMF is equilibrated through outward advection and magnetic-quenching (i.e., we artificially increased the coefficient of the magnetic diffusion in the TL to allow a flux-loss of the TMF). In the TL, one possible solution for the radiative MHD equations is a self-similar solution in which the variables obey the following power-laws:

$$\Omega \sim r^{-5/4}, \rho \sim r^{-3/2}, T_i \sim r^{-1/2}, U_r \sim r^{-1/4}, B_p/B_T \sim \text{const.} = \epsilon, \quad (15)$$

where $\epsilon = H_W/r$, and H_W is the width of the TL. The most prominent properties of this solution are:

1. The ratio of heating to advection time scale of the ions is of order unity, i.e., $\tau_h/\tau_{\text{adv}} \approx 1$. The ratio of heating to Coloumb-cooling time scale of the ions is: $\tau_h/\tau_{\text{Coul}} \sim r^{-1/2}$. This implies that thermal coupling between electrons and ions diverges with distance from their origin, and gives rise to multi-component jet-plasma. Furthermore, ions cool pre-dominantly through advection, i.e., adiabatic expansion.
2. The ratio of the amplification of the TMF to the flux-loss time scale is of order unity. The same applies to the ratio of the advection to amplification time scale. Thus, This implies that a significant fraction of the toroidal magnetic flux is advected outwards, and which thereafter acts to collimate the flow. On the other hand, the magnetic diffusivity in the TL scales: $\eta_{\text{mag}} \approx H_W(B_p/B_T)V_\varphi \sim \epsilon r^{3/4}$. This η_{mag} — description must break down at a certain radius r_{col} , where η_{mag} becomes negligibly small and collimation starts to be efficient.
3. The rate of the outward-oriented material flux in the TL reads:

$$\dot{\mathcal{M}}_W(r) = \dot{\mathcal{M}}_W(r = r_{\text{in}}) + \epsilon^2 \dot{\mathcal{M}}_d(r = r_{\text{in}}) \left(\left(\frac{r}{r_{\text{in}}} \right)^{1/4} - 1 \right), \quad (16)$$

where $\dot{\mathcal{M}}_W(r = r_{\text{in}})$ and $\dot{\mathcal{M}}_d(r = r_{\text{in}})$ are the wind-flux rate and the disk accretion rate at the inner boundary. Thus, the wind flux increases with radius, although it is a rather weak dependence.

4. the associated angular momentum flux with the wind increases linearly with distance from the central BH:

$$\dot{\mathcal{J}} = \text{const. } r, \quad (17)$$

which implies for $r \leq r_{\text{tr}} \approx 10 - 20 R_{\text{LSO}}$.

The global energy distribution in the disk and jet region can be well represented by the Bernoulli number (Be). Flows with total positive energy are gravitationally unbound, and potentially they may propagate to infinity, whereas flows with negative total energy are gravitationally bound and they end their motion inside the BH. If the flow, however, is dissipative, energy exchange between different parts of the flow is possible, which gives rise to inflow-outflow configurations. Fig. 9, for example shows that Be is everywhere negative safe the TL, where it attains large positive values.

We note that the outflow is sufficiently strong to shift the PMF lines outwards, whereas the large magnetic diffusivity prevents the formation of large electric currents along the equator. In the case of weak MFs ($\beta \leq 0.1$), our calculations reveal rather weak outflows, which is reasonable, since a low β yields a longer τ_{TAW} , which may become longer than the dynamical time scale. Moreover, low β s inflows force MFs to establish a monopole like-topology (i.e, a one-dimensional MF-topology which is not appropriate for producing strong TMFs). In this case, the rate of TMF-generation is considerably reduced. TAWs become inefficient at magnetic-braking the disk, reducing therefore the power required for launching jets. This indicates that weakly magnetized disks are in-appropriate for launching powerful jets, and that magnetized accretion flows are more suited for jet-production than their HD-counterparts. Comparing the flux of matter in the wind region to that in the disk, it has been found that $\dot{M}_W/\dot{M}_d = \text{const.} \sim \epsilon^2$. The angular momentum flux associated with the wind is $\dot{J}_W/\dot{J}_d = a (\dot{M}_W/\dot{M}_d) r^{1/4}$, where "a" is a constant of order unity. Consequently, at 500 gravitational radii almost 15% of the total accreted angular momentum in the disk re-appears in the wind. To clarify why the TL is geometrically thin, we note that the ratio:

$$\frac{\tau_{\text{TAW}}}{\tau_{\text{adv}}} \sim \left(\frac{r}{H_d}\right) \left(\frac{V_A}{U}\right) \sim \frac{r}{H_d} > 1, \quad (18)$$

where τ_{adv} is the advection time scale. The last inequality implies that angular momentum in the TL will be advected outwards more efficiently than being extracted through TAWs to higher latitudes. Furthermore, since the flow in the TL is highly dissipative, TMF-lines tend to close in the TL, thereby considerably reducing the efficiency of angular momentum transport to much higher latitudes. Also, as the flow in the TL rotate super-Keplerian, the normal component of the centrifugal force tend to shift the matter towards the equator.

On the other hand, the corona above the TL has been found to be dynamically unstable. Unlike normal stars that heat up the surrounding corona from below, in the absence of other energy sources, black holes cannot supply the surrounding corona with heat, hence they start to collapse dynamically.

To elaborate this point, let us compare the conduction time scale with the dynamical time scale along B_p-field at the last stable orbit of a SMBH:

$$\frac{\tau_{\text{cond}}}{\tau_{\text{dyn}}} = \frac{r\rho U_r}{\kappa_0 T_i^{5/2}} = 4.78 \times 10^{-4} \rho_{10} T_{i,10}^{-5/2} \mathcal{M}_8,$$

where ρ_{10} , $T_{i,10}$ and \mathcal{M}_8 are respectively in $10^{-10} \text{ g cm}^{-3}$, 10^{10} K and in $10^8 \mathcal{M}_\odot$ units. This is much less than unity for most reasonable values of density and temperature typical for AGN-environments. In writing the above equation we have optimistically taken the upper limit $c/\sqrt{3}$ for the velocity, and set $\kappa_0 = 3.2 \times 10^{-8}$ for the ion-conduction coefficient. When modifying the conduction operator to respect causality, we obtain $\tau_{\text{cond}}/\tau_{\text{dyn}} \leq U_r/c$, which is again smaller than unity.

This agrees with our numerical calculations which rule out the possibility of outflows from the corona, and in particular not from the highly unstable polar region of the BH, where matter is neither magnetic- nor centrifugal-supported against the central gravity of the BH.

7 Formation of electron-proton jets: summary

In this paper we have presented a model for initiating jets from systems containing BHs surrounded by accretion disks. The model is based on the following sub-structures:

1. A weakly magnetized accretion disk in the outer region. Balbus-Hawley instability amplifies the weak MFs up to thermal equipartition which, in combination with the Parker instability and inward-advection of matter, re-generate a PMF of large scale topology. This large scale PMF turns the disk at r_{tr} into advection-dominated. However, since this occurs on the dynamical time scale which is radius-dependent, r_{tr} is basically the outer boundary, or alternatively is close to the last stable orbit. The former possibility is observationally inconsistent, as this would force the disk to truncate at large radii and terminate accretion. The later possibility is plausible: assume the flow at r_{tr} is freely falling, and has the vertical width of $H_d/r = 1/30$. Using $\rho(r, \theta = 0) = \rho(r_0, \theta = 0)(r_{\text{BL}}/r)^{3/2}$ and $B_p(r, \theta = 0) = B_p(r_0, \theta = 0)(r_{\text{BL}}/r)^2$, one can easily find that MFs would terminate accretion if $r_{\text{tr}} \geq 16 r_{\text{LSO}}$, where r_{LSO} is the last stable radius. Here we have assumed that whatever the strength of the MF is, the magnetized inflow interior to r_{LSO} is gravitationally bound and will be accreted, together with the MF, into the hole. In this region, we anticipate large scale MFs to change into a monopole like-topology. Thus, an advective disk threaded by large scale MFs must be located inside $10 - 20 r_{\text{LSO}}$, depending on the accretion rate.
2. In the region $r_{\text{top}} \leq r \leq r_{\text{tr}}$, TAWs are the dominant angular momentum carrier. The transport proceeds vertically and on the dynamical time scale, which requires the disk, again, to be advection-dominated for stably supplying the jet with angular momentum. The angular momentum associated with TAWs is deposited in the turbulent-diffusive TL between the disk and the corona, where vast of the shear-generated TMFs reconnect and heat the ions up to the

virial temperature. Beside the fact that the large magnetic-diffusivity in the TL lengthens the time scale of TAWs to cross the TL compared to the local dynamical time scale (; necessary for maintaining a geometrical thin TL), reconnection of the TMF-lines terminates magnetic braking and yields a trapping of the angular momentum. Consequently, the virial-heated ions are then forced to rotate super-Keplerian and centrifugal-accelerate outwards.

Another argument in favor of the thin geometrical structure of the TL is that the corona is thermally unstable. The reasons are: 1) absence of heating from below, 2) centrifugal forces are weak, and 3) Lorentz forces exerted on the plasma in the polar region of the BH are negligibly small.

3. The plasma in the TL is tenuous, highly advective, two-temperature and ion-dominated, which gives rise to the formation of electron-proton jets. The shear-generated TMFs in the TL are in thermal equipartition with the ions and in super-equipartition with the thermal energy of the electrons. Such a strong TMF in the TL is necessary for explaining the observed excess of radio luminosities such as in M87 and GRO 1655-40.
4. Since the pressure-gradient vanishes at the horizon, a rarification wave starts to move from inside-to-outside, leaving the matter behind its front free-falling. The resulting density profile has a global maximum at $r_{\text{BL}} (\ll r_{\text{tr}})$, and a minimum at the inner boundary r_{in} , where the dynamical time scale is shortest, and where the strength of Coulomb coupling between the ions and electrons is weakest. Consequently, the disk truncates at r_{BL} and an highly advective ion-dominated torus emerges in the BL. The MF in the ion-torus change topologically from large scale into monopole. Such a change is associated with a significant loss of magnetic flux in the hole, which is necessary for preventing magnetic termination of accretion.
5. When does the outflow start to collimate into jet?

A significant part of the shear-generated TMFs reconnect in the TL and heat the ion preferentially. The other part is advected outwards with the plasma on the dynamical time scale. Inspection of Equation 1 shows that the ratio of the viscous to the advective time scale of angular momentum in the TL reads:

$$\frac{\tau_{\text{visc}}}{\tau_{\text{adv}}} \approx \frac{rV_{\text{A}}}{\nu_{\text{tur}}}. \quad (19)$$

In writing this approximation we have inserted $V_{\text{A}}^{\text{T}} = B_{\text{T}}/\sqrt{\rho} = V_{\varphi}$, which is applicable for the plasma in the TL. Therefore, given the critical radius $r_{\text{col}} (\doteq \nu_{\text{tur}}/V_{\text{A}})$ at which both viscous and advective time scale are equal, collimation will start for $r \geq r_{\text{col}}$. This is easy to fulfil, as V_{A} increases with distance from

the BH, or remain constant, whereas ν_{tur} must decrease. This gives rise to extremely large ratio of $\tau_{\text{visc}}/\tau_{\text{adv}}$. Therefore, beyond r_{col} , particle-trajectories of motion is dictated by MFs.

Finally, the model is similar to the Blandford & Znajek (1977) scenario, as vertical transport of angular momentum by TAWs is mediated almost without advection of matter. This gives rise to high collimated and extremely low mass load jets. The global configuration of the jet-disk connection presented in this paper enhance the role of the central engine in powering the jet. A spinning BH will likely feed the jet with extra rotational energy through the frame dragging effect, whereas a non-rotating hole may have the opposite effect: extraction of energy from the plasma in the TL, hence a less powerful jet.

Additionally, the model may provide explanations for several other important issues related to the formation of jets and disks: 1) the $K\alpha$ emission lines observed in Cyg X-1 which suggest that the disk-plasma in the vicinity of the last stable orbit is cold and rotates Keplerian, 2) The origin of the super-Keplerian motions observed in the Galactic black holes XTE J1650-500 and MCG-6-30-15 [22], which suggest that the central objects are spinning BHs, and 3) the origin of the extremely low mass-load jets observed in several AGNs and μ -quasars.

References

- [1] Abramowicz, M., Igumenshchev, I., Lasota, J-P., MNRAS, 293, 433, (1998)
- [2] Balbus, S., Hawley, J., ApJ, **376**, (1991)
- [3] Biretta, J., Junor, W., Livio, M., New Ast. Reviews, **46**, 239, (2002)
- [4] Blandford, R., Znajek, R., MNRAS, 179, 433, (1977)
- [5] Blandford, R., Payen, D., MNRAS, 199, 883, (1982)
- [6] Blandford, R., Begelman, M., MNRAS, 303, L1, (1999)
- [7] Blandford, R., astro-ph/0110394, (2001)
- [8] Camenzind, M., RvMA, 3, 234, (1990)
- [9] Di Matteo, T., Allen, S., Fabian, A., et al., ApJ, 582, 133, (2003)
- [10] Esin, A., McClintock, J.E., Drake, J., et al., ApJ, 555, 483, (2001)
- [11] Hawley, F., Gammie, C., Balbus, S., ApJ, **464**, 690, (1996)
- [12] Heyvaerts, J, Norman, C., ApJ, 347, 1055, (1989)

- [13] Hujeirat, A., Camenzind, M., A&A, **361**, L53, (2000a)
- [14] Hujeirat, A., Camenzind, M., A&A, **362**, L4, (2000b)
- [15] Hujeirat, A., Rannacher, R., New Astro. Reviews, 45, 425 (2001)
- [16] Hujeirat, A., Camenzind, M., Burkert, A., A&A, 386, 757, (2002)
- [17] Hujeirat, A., Camenzind, M., Livio, M., A&A, **394**, L9, (2002)
- [18] Hujeirat, A., in preparation, (2003)
- [19] Ghosh, P., Lamb, F.K., ApJ, 223, 83, (1978)
- [20] Lovelace, R., Berk, H., Contopoulos, J., ApJ. 379, 696, (1991)
- [21] Königl, A., ApJ, 342, 208, (1989)
- [22] Miller, J.M., Fabian, A.C., Wijnands, R., ApJ, 570, L69, (2002)
- [23] Mirabel, I.F., Astroph/0005591, (2000)
- [24] Mirabel, I.F., ApSSS, **276**, 153, (2001)
- [25] Narayan, R., Yi, I., ApJ, **444**, 231, (1995)
- [26] Ogilvie, I., Livio, M., ApJ, **553**, 158, (2001)
- [27] Popham, R., Sunyaev, R.A., ApJ, 547, 355, (2001)
- [28] Pudritz, R., Norman, C., ApJ, 274, 677, (1983)
- [29] Paczyanski, B., Wiite, P.J., A&A, 88, 23, (1980)
- [30] Rees, M., Begelman, M., Blandford, R., & Phinney, E., Nature, **295**, 17, (1982)
- [31] Rybicki, G., Lightman, A.P., Radiative processes, Wiley-Interscience Publication, (1979)
- [32] Shakura, N. I., Sunyaev, R. A., A&A, **24**, 337, (1973)
- [33] Sandbæk, O., Leer, E., ApJ, 423, 500, (1994)
- [34] Shu, F., Lizano, S., Ruden, S., Najita, J., ApJ, 328, L19, (1988)
- [35] Shu, F., The Physics of Star Formation and Early stellar Evolution, ed. Kylafis, N.D., & Lada, C.J., Dordrecht: Kluwer), 365, (1991)

- [36] Shu, F., Najita, J., Ruden, S., Lizano, S., ApJ, 429, 781, (1994)
- [37] Simon, T., ASP, 223, 235, (1999)
- [38] Spiegel, E., Zahn, J.-P., A&A, 265, 106, (1992)
- [39] Stone, J.M., Pringle, J.E., Astrph/0009233, (2000)
- [40] Tout, C.A., Pringle, J.E., MNRAS, 259, 604, (1992)
- [41] Uchida, Y., Shibata, K., PASJ, 37, 515, (1985)
- [42] Yuan, F., Markoff, S., Falke, H., 383, 854, (2002)

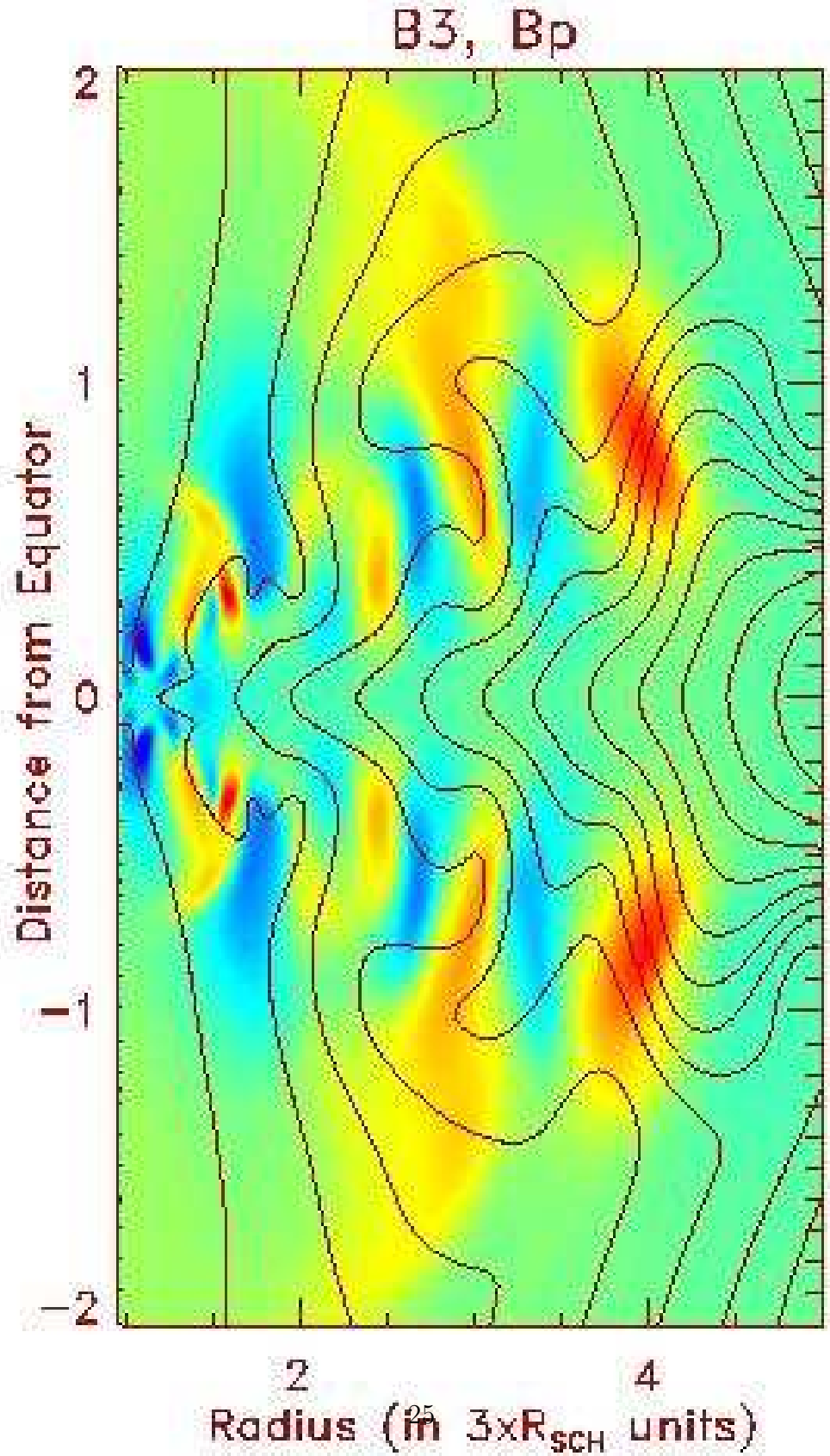


Figure 7: The distribution of 30 weak PMF-lines around a non-rotating BH (black lines), superposed on TMF-distribution (blue corresponds to large positive values, and red to negative values). In this run we set $\beta = 1/20$, the disk is relatively hot

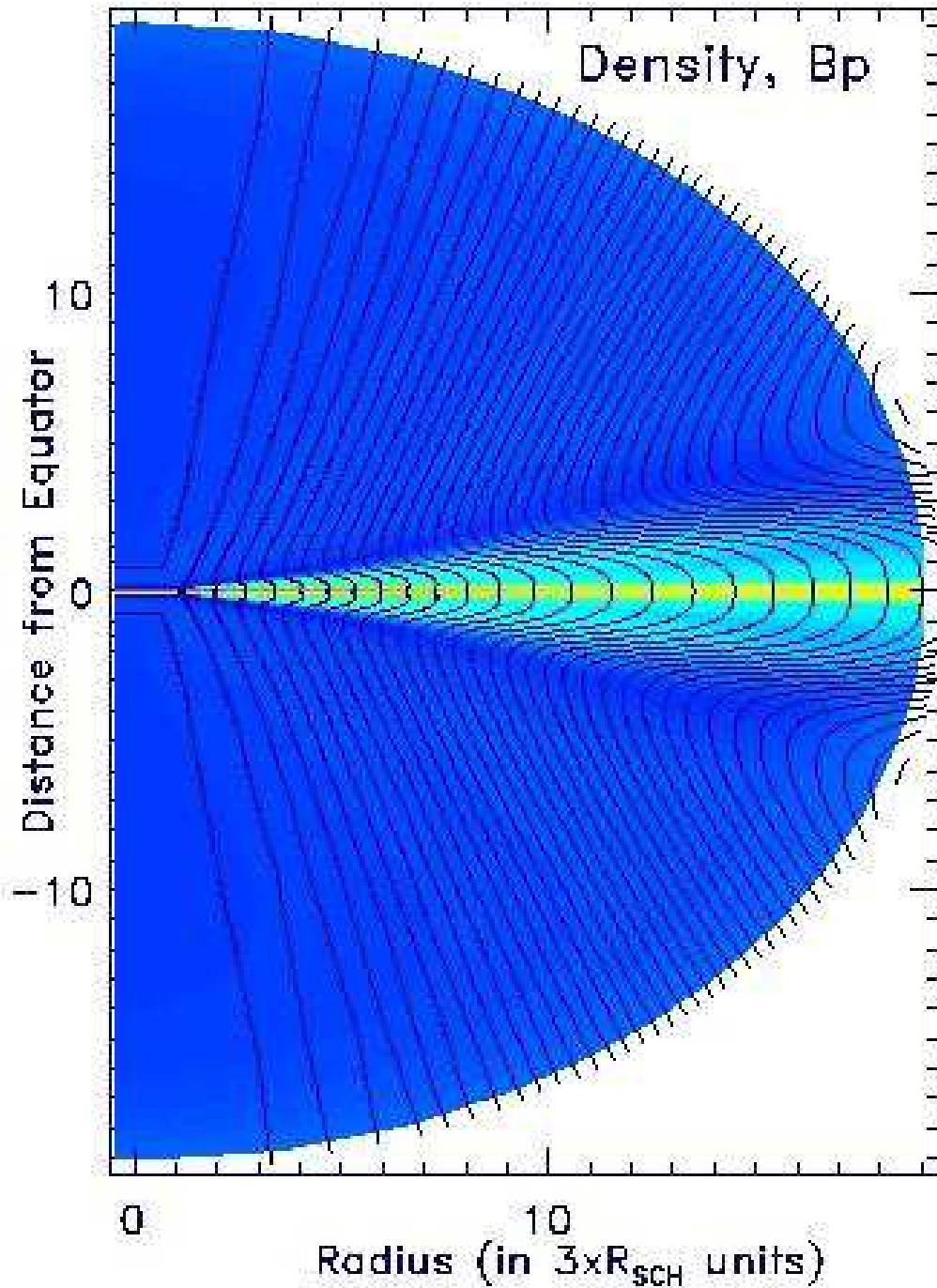


Figure 8: 30 equally-spaced isolines of the poloidal-component B_p (black lines) and the density-distribution (yellow color corresponds to very high density-values, blue to middle and violet to low values).

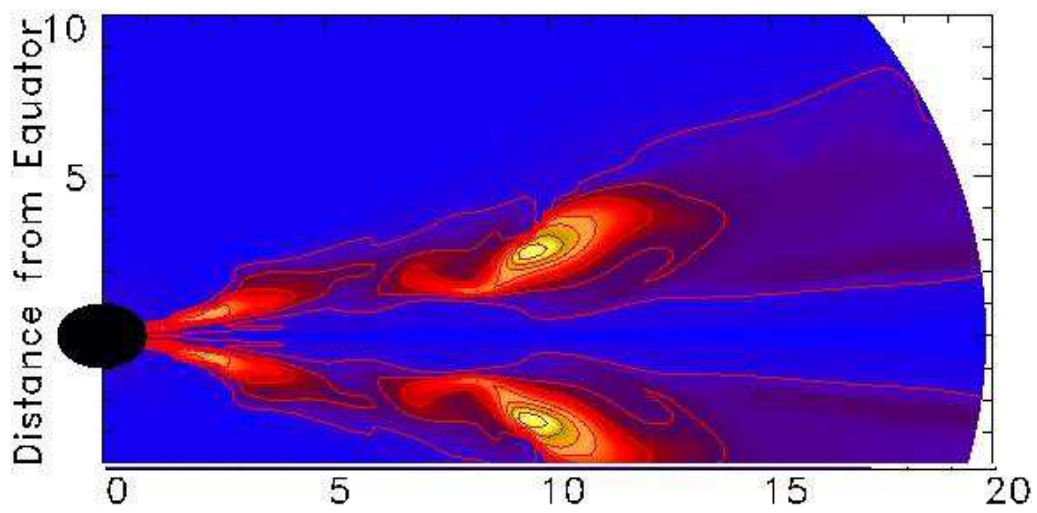


Figure 9: A snap-shot of the distribution of the Bernoulli number in two-dimensional quasi-stationary calculations. The decrease from large to low positive values is represented via yellow, green and red colors. The blue color corresponds to negative values. The figure shows two ejected gravitationally unbound blobs of large positive energies in the TL.

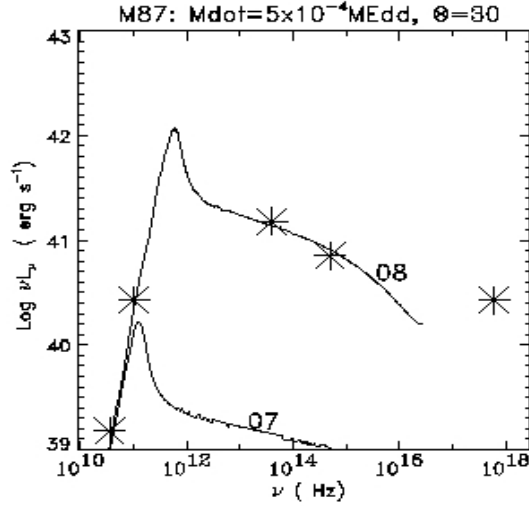


Figure 10: The SED of a disk-jet model of the elliptical galaxy M87. Similar to Biretta 2002 and Di Matteo 2003, an accretion rate of $5 \times 10^{-4} \dot{M}_{\text{Eddington}}$ and $T = 5 \times 10^6 \text{K}$ is set to enter the domain of calculations through the outer boundary which is located at 150 Schwarzschild radii from the central SMBH. The vertical scale height of the disk at the outer boundary is taken to be $H \approx 0.1 R_{\text{out}}$. Additionally, a hot tenuous corona is set to sandwich the optically thin disk. The calculated profiles (solid lines) are superposed on the observational data (asterisks). The line 07 corresponds to a model in which the PMF is set to be in equipartition with the thermal energy, whereas $\text{TMF}=0$. The line 08 is similar to 07, but the TMF is allowed to develop and reach values beyond equipartition with respect to the thermal energy of the electron in the TL. The above SED has been obtained by solving the radiative transfer in 4-dimensions, taking into account the Kompaneets equation for consistently modelling Comptonization (see [16],[18] for further details).